Semi-Cutting-Assisted Laser Welding of Zinc-Coated Steels in a Zero Root Opening, Lap-Joint Configuration

High-quality, zero root opening laser welds (4.8 m/min) in zinc-coated steels in a lap-joint configuration were achieved

BY S. YANG, Z. CHEN, W. TAO, C. WANG, J. WANG, AND B. E. CARLSON

ABSTRACT

Because of their excellent corrosion resistance, zinc-coated steels have been widely used in the automotive industry. However, the generation of highly pressurized zinc vapor during the laser beam welding process presents unique challenges for body manufacturing. In this study, a semi-cutting-assisted laser welding process was developed to weld zinc-coated steels in a zero root opening, lap-joint configuration using a specially designed nozzle for delivery of the shielding gas. Effects of welding speed on the weld quality were investigated, resulting in high-quality welds being achieved at a relatively high welding speed of 4.8 m/min. The success in achieving high-quality, zinc-coated steel welds by semi-cutting laser welding is attributed to an improved drag force. This, in turn, is a result of the increased shielding gas flow rate, which enlarges and stabilizes the keyhole, enabling the zinc vapor to escape from the faying interface of the two metal sheets. Tensile shear and microhardness tests were conducted to evaluate mechanical properties of the welds. Optical microscopy was also used to examine the microstructure of the welds. It was demonstrated the weld strength was comparable to the base metal.

KEYWORDS

• Zinc-Coated Steels • Lap-Joint Configuration with Zero Root Opening • High-Speed Welding • Shielding Gas Flow Rate • Weld Discrepancies • Keyhole

Introduction

Zinc-coated steels provide excellent corrosion resistance for automotive body structural and closure components. In addition, zinc-coated steels also enhance the production stamping performance. These features genuinely drive increased usage of zinc-coated steels in the automotive industry. However, one of the most significant challenges for implementing zinc-coated steels is to weld the zinc-coated steels, especially in a lap-joint configuration, without producing weld discrepancies. Compared to the melting point of steel (over 1500°C), zinc has a significantly lower boiling point, 906°C. During the laser welding process, a highly pressured zinc vapor is readily produced, which often leads to the formation of various discrepancies, including weld spatter and porosities. Because of the aforementioned weld discrepancies, mechanical performance of the welds is dramatically reduced. Therefore, steps must be taken with regard to the welding process in order to suppress the zinc vapor. Unfortunately, this increases the manufacturing complexity and reduces productivity.

With respect to productivity and flexibility, laser welding has many advantages compared to other welding processes. In the past several decades, different laser welding techniques have been proposed to weld zinc-coated steels in a lap-joint configuration. These laser welding techniques can be categorized by the following:

1. Setting a prescribed root opening size of 0.1–0.2 mm at the faying interface of metal sheets prior to the welding process (Refs. 1, 2).

The root opening can be created by a stamping process, mechanical methods, as well as a laser beam. The root opening created provides a lateral channel for the highly pressurized zinc vapor to escape from the interface before the steel around the interface is melted. Consequently, the formation of spatter can be avoided. However, an inconsistent root opening could lead to the formation of weld discrepancies such as undercutting and porosity. Recently, a remote laser-welding process has been used to weld three zinc-coated steel sheets in a lap-joint configuration (Ref. 3). Experimental results demonstrated that with an optimized root opening size, acceptable welds could be achieved in a three-sheet stackup of zinc-coated steel sheets although porosity was still generated within the welds (Ref. 3).

2. Enlarging the molten pool and thereby extending the solidification time with the use of a second heat source, providing sufficient time for the zinc vapor to escape from the

S. YANG (david.s.yang@gm.com) *is a senior researcher, W. TAO is an associate researcher, and J. WANG is a lab group manager with China Science Lab, General Motors Global Research & Development Center, China. Z. CHEN is a master student and C. WANG is a professor with Huazhong University of Science and Technology, China. B. e. Carlson is lab group manager with General Motors research & Development Center, Warren, Mich.*

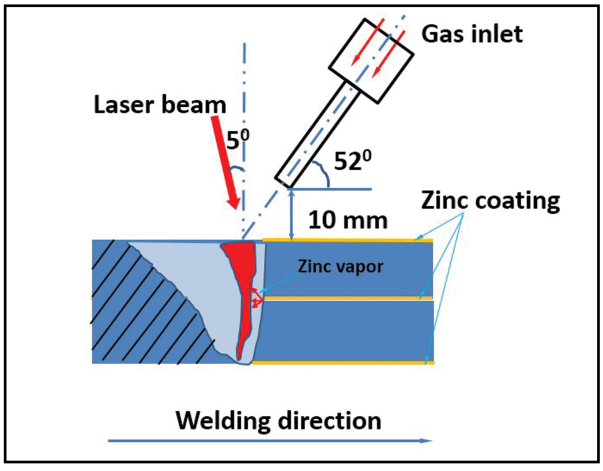

Fig. 1 — Schematic of experimental setup with semi-cutting-assisted laser welding.

molten pool and keyhole (Refs. 4–7).

The molten pool can be enlarged by combining a laser beam with an arc or second laser beam that share a common molten pool. With a longer solidification time, the zinc vapor has a greater possibility to escape through the molten pool. The main constraints of these techniques are imposed by the limited space available in the production welding cell in addition to the relatively high capital investment needed for two heat sources as well as complex operation.

3. Cutting a slot by a laser beam along the weld interface prior to laser welding (Refs. 8–11).

Another possibility is to cut a slot by a precursor laser beam in order to provide an exit path for the zinc vapor and the welding process is carried out by a second laser beam (Ref. 9). The slot size used in this method is a function of the welding speed and the metal sheet stack-up thickness. The narrow bonded area at the faying interface of the metal sheets could reduce the weld strength.

4. Modification of the zinc composition by addition of a second alloying element such as copper or aluminum (Refs. 12, 13) or replacement of the zinc coating at the faying surface by a nickel-based coating (Refs. 14, 15).

The compounds of zinc-copper and zinc-aluminum as well as nickel have melting points higher than the boiling point of zinc. Therefore, use of these materials would reduce or avoid the generation of zinc vapor resulting in a more stable welding process. The negative aspect of these methods is that they add extra process steps and the material compositions could act to reduce the weld mechanical properties caused by excessive dissolution of aluminum or copper into the welds.

Table 1 — Chemical Composition of Low-Carbon Steel (wt-%)

Steel	C	Mn	P	Si	S	Al	Cr	Ca	Ti
	≤0.006	≤0.2	≤0.025	_	≤0.02	≥0.015	_	_	0.03/0.08

5. Laser welding assisted by arc or laser preheating (Refs. 16–18).

Use of a preheat source causes the zinc coating on the top surface of the workpieces to be vaporized and a portion of the zinc coating at the faying interface is converted into zinc oxide. The advantage of zinc oxides is that they have a significantly higher melting point than the boiling point of zinc (1975° vs. 906°C). Therefore, when the following laser beam comes into position for welding, there is significantly less zinc available to generate the deleterious zinc vapor, stabilizing the molten pool and keyhole, which further helps any remaining zinc vapor escape, thereby achieving defect-free welds.

6. Optimization of shielding gas (Refs. 19, 20). The laser-induced plasma can be suppressed and the interaction between zinc vapor and laser beam can be reduced through optimization of the shielding gas for improved coupling of the laser beam energy. Furthermore, the addition of oxygen into the shielding gas can increase weld penetration and stabilize the keyhole, which results in an improved weld quality of zinc-coated steels (Ref. 19).

7. Pulsed laser welding (Ref. 21).

A stable keyhole can be achieved by optimizing pulsed laser welding parameters, including the peak power, duty cycle, travel speed, pulse repetition rate, and pulse energy. The optimization is focused on allowing the zinc vapor to be mitigated and achieving visually sound welds. However, typically a large amount of porosity is retained within the weld using this method. Another limitation for this method is the relatively low welding speed, which limits its application.

8. Laser welding assisted by vacuum (Ref. 22).

This relatively new process uses a suction device to create a negative pressure zone (relative to ambient) directly above the molten pool. The purpose of this negative pressure zone is twofold. Firstly, a drag force is generated due to the external suction device, which can counterbalance the shear force induced by the erupting zinc vapor. Secondly, the negative pressure zone facilitates the zinc vapor to escape along the suction direction. As a result, the molten pool becomes more stable and the keyhole will remain open and allow the escape of zinc vapor. Defect-free, zinc-coated welds were achieved using this method, but it requires ancillary vacuum equipment to be introduced into the production cell.

Although the methods mentioned above achieve technically acceptable weld quality, there are constraints associated with each of these methods, which inhibits the full implementation in production. Furthermore, laser welding speeds of more than 3 m/min are needed in order to meet typical productivity requirements. Currently, there is limited published literature in the area of laser welding of zinc-coated steels at speeds greater than 3 m/min.

In this study, a semi-cutting-assisted laser welding process was developed (Patent Reference Number: GMC-338-A-CN) to weld zinc-coated steels in a zero root opening, lap-joint configuration. Here, the semi-cutting-assisted laser welding is referred to as a defined laser welding process where a gas jet with relatively higher gas flow velocity than that in the conventional laser welding process is used to increase the fluid flow transfer rate in the molten pool. Instead of using a conventional shielding gas with a relatively large diameter equal to or larger than 6 mm, a smaller shielding gas nozzle of 2 mm diameter was used. To better understand the effect of welding speed on the weld quality, experiments were carried out at welding speeds of 3, 4.2,

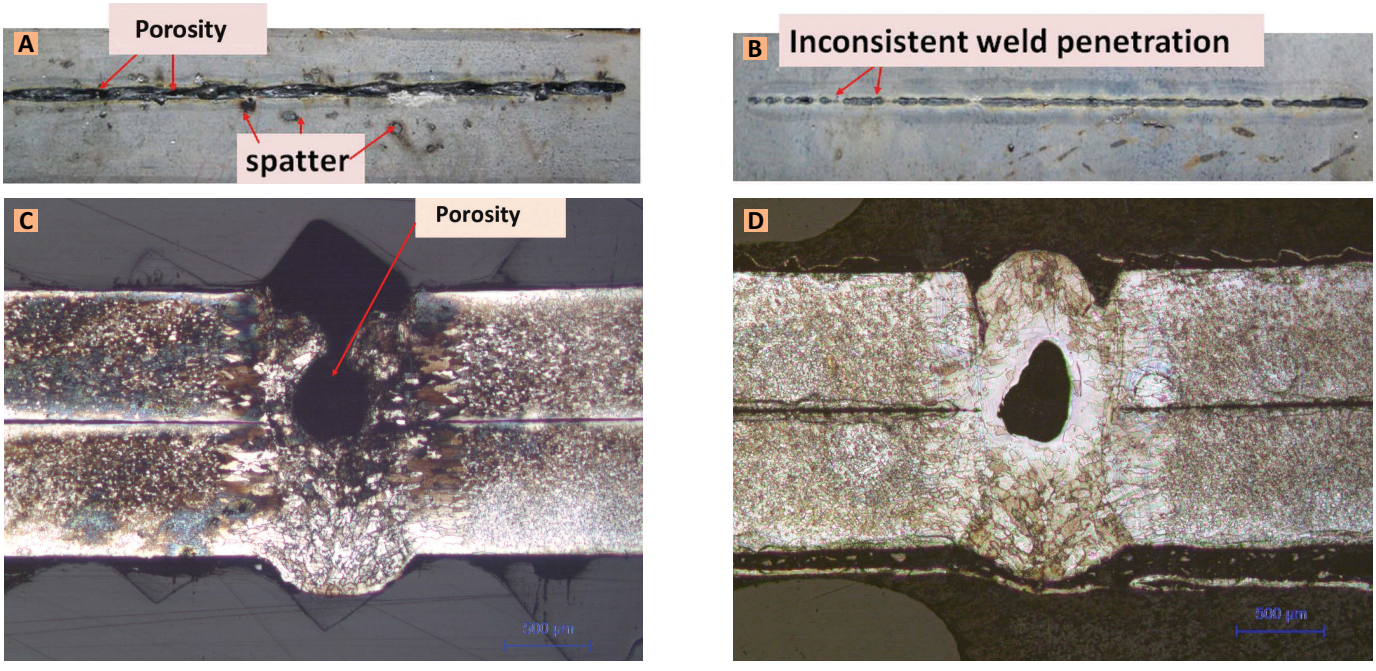

Fig. 2 — Typical characteristics of the welds obtained by a conventional laser welding process. A — Top view; B — bottom view; C — cross-sectional view of porosity; D — porosity produced inside the weld.

and 5.4 m/min. High-quality welds were achieved by using this new laser welding technique. In addition, tensile shear and hardness tests were performed to evaluate mechanical properties of the welds.

Experimental Procedures

Materials

Zinc-coated, low-carbon steel was chosen for this research. The specimen dimensions of the workpiece were 120 × 85 × 0.8 mm. The zinc coating was hot-dip galvanized at a level of 60 g/m^2 per side. Prior to welding, the surfaces of the steel plates were cleaned with alcohol in order to remove any dirt on the surface of the workpiece that may interfere with clamping of the workpieces.

Table 1 lists the chemical composition of the low-carbon steel used in this study.

Laser Welding Procedure

The laser beam welding experiments were conducted using an IPG YLS-4000 fiber laser (wavelength: 1070 nm; focal length: 250 mm; focal spot diameter: 0.3 mm). Pure argon was used as the side shielding gas. The two steel plates were tightly clamped together prior to laser welding, and it is assumed that no root opening existed between the two metal plates.

A 2-mm-diameter shielding gas nozzle of made of a copper alloy was designed and applied in this study, schematically shown in Fig. 1. As shown in Fig. 1, the stand-off distance of the shielding gas nozzle was 10 mm, which is an order of magnitude larger than that typically used for laser cutting. For conventional laser cutting, the laser cutting header is perpendicular to the workpiece, and the stand-off distance between the nozzle and the workpiece is selected in the range between 0.5 and 1.5 mm (Ref. 23). Furthermore, the nozzle was set at an inclination angle of 52 deg with respect to the upper workpiece top surface. During the laser welding process, the shielding gas nozzle is positioned such that it is in front of the laser beam. The laser beam itself has an inclination angle of 5 deg with respect to the vertical direction, i.e., normal to the upper workpiece surface, in order to avoid backreflection from the laser light. The gas flow velocity at the exit of the shielding gas nozzle can be calculated by the equation: flow rate/cross-sectional area of the shielding gas nozzle. Assuming that the shielding gas flow rate from the storage container to the exit of the shielding gas nozzle is kept constant, the gas-flow velocity used in this study is about 66m/s

$$\left(v = \frac{flow\ \ rate}{cross-sectional\ \ area\ \ of\ \ used\ \ nozzle} = \frac{0.75 m^3/h}{\pi \times 1^2} \right).$$

During the laser welding process, the gas pressure is kept constant and the temperature of the shielding gas is assumed to be at room temperature.

Metallography and Microhardness Test

The laser-welded lap joint was sectioned perpendicular to the weld joint direction. This cross section was then cut, mounted, ground, polished, and etched as a precursor to microhardness measurements. Vickers microhardness tests were conducted using a load of 100 g and a dwell time of 10 s. In addition, optical microscopy was applied for microstructural examination.

Tensile Shear Test

Tensile shear test samples were prepared according to the sheet type of ASTM-E8/E8 M-08 standard (gauge length: 50 mm). Tensile shear tests were conducted in uniaxial tension using a 3-kN load cell. The model

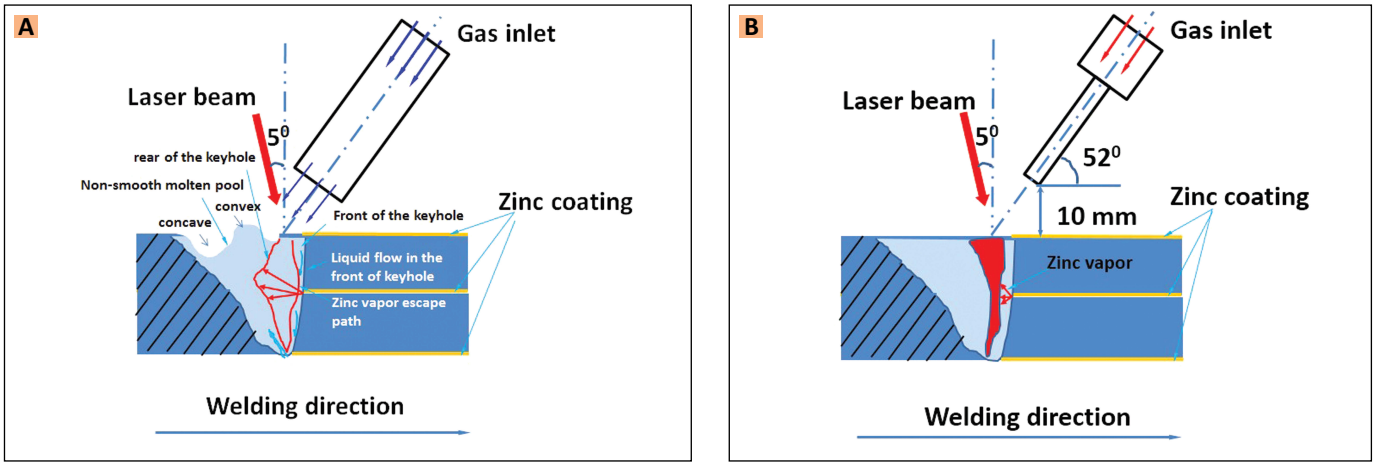

Fig. 3 — Schematic comparison. A — Conventional laser welding; B — semi-cutting-assisted laser welding.

number of the tensile testing machine is QJ-211. All tests were run at ambient temperature and a constant crosshead velocity of 2 mm/min. Three replicates were conducted for each welding condition, and the average peak load was calculated.

Results and Discussion

Semi-Cutting-Assisted Laser Welding

A highly pressurized zinc vapor is readily produced at the faying surface during laser welding of zinc-coated steels in a zero root opening, lap-joint configuration. The zinc vapor quickly expands inside the molten pool and disrupts both the molten pool and keyhole — Fig. 3A. This disruption is, in part, rippling of the molten pool surface where different types of rippling having various magnitudes are observed during the laser welding process. The rippling fluctuates in the form of waves at high frequency and magnitude, and reflects most of the laser beam energy from the surface of the molten pool (Ref. 22). As a consequence, the coupling of the laser-beam energy into the workpiece is dramatically reduced and the weld penetration depth becomes shallow. Furthermore, in the worse situation, the liquid metal in the molten pool moves along the welding direction and collapses the keyhole. The collapsed keyhole entraps the zinc vapor, which quickly expands inside the molten pool. Under these welding conditions, liquid metal is ejected out of the molten pool in the rear of the keyhole as the zinc vapor reaches the molten pool surface.

The ejected liquid metal condenses in the air and deposits on the top surface of the workpieces, resulting in the formation of spatter — Fig. 2A. If the liquid metal cannot fill in the cavity caused by the loss of the ejected liquid metal in a timely manner, then porosity is produced in the welds (Ref. 7) — Fig. 2A, C. This phenomenon was observed to occur intermittently. After the highly pressurized zinc vapor is released, the molten pool becomes relatively stable. However, when the zinc vapor pressure level builds to some threshold, the molten pool again becomes unstable. The presence of these weld discrepancies dramatically reduces the weld strength.

Figure 2A shows typical weld features obtained by conventional laser welding. As shown in Fig. 2B, inconsistent weld penetration is usually observed in the welds.

In order to suppress the zinc vapor, a new laser welding process was proposed to weld zinc-coated steels in a zero root opening, lap-joint configuration where an innovative nozzle was designed to simultaneously create a semi-cutting action in addition to a laser welding process. This newly developed method is hence forth referred to as the semi-cutting-assisted laser welding process. As shown in Fig. 3B, a much smaller 2-mm-diameter shielding gas nozzle was used instead of the regular shielding gas nozzle with a diameter with equal to or greater than 8 mm. Compared to conventional laser welding, the narrower nozzle size used in the semi-cutting-assisted laser welding process reduces the coverage area of shielding gas on the workpiece, thus increasing the possibility of the weld oxidation. However, oxidation of a laser weld with a width of about 1–6 mm can be prevented by the divergence of shielding gas even when using a smaller nozzle with a diameter of about 2–6 mm.

In this study, the weld size is about 1.0 mm in Fig. 4 and can be fully covered by the smaller nozzle. Because of the reduced cross-sectional area of the nozzle, the velocity of the shielding gas was dramatically increased. When the nozzle diameter is reduced from 8 to 2 mm, the velocity of the shielding gas is increased by 16 times since the velocity of shielding gas is inversely proportional to the square of the nozzle diameter. This way, a straight and nonturbulent gas jet having greater momentum is created that when applied during the laser welding process creates a higher drag force exerting on the molten pool and keyhole. As a consequence, the mass transfer rate of the molten liquid from the front of the keyhole to the molten pool behind the keyhole is increased due to the increased pressure from the higher velocity gas jet used in the semi-cutting-assisted laser welding. Furthermore, the surface tension force that tends to close the keyhole is encountered.

The drag force (F_d) exerted on top of the molten pool and the keyhole can be determined by Newton's equation for drag force:

$$F_d = C_d\left(\frac{\pi d}{4}\right)\left(\frac{\rho_g v^2}{2}\right) \quad (1)$$

where ρ is the density of the gas (kg

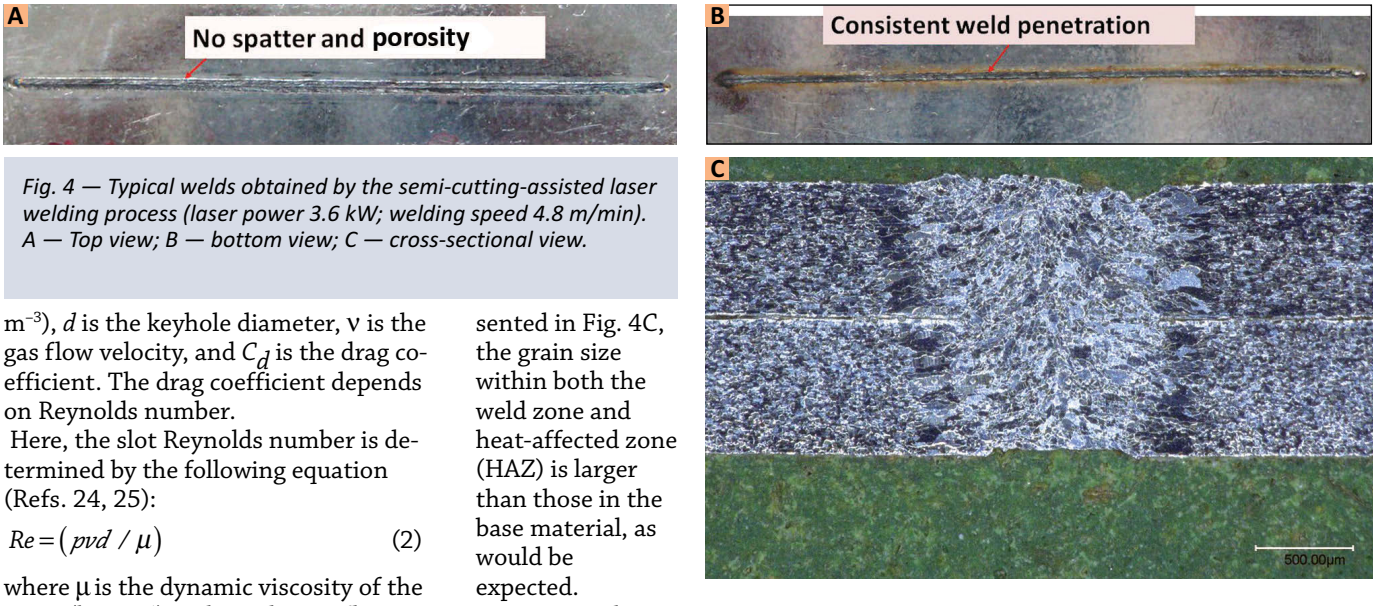

Fig. 4 — Typical welds obtained by the semi-cutting-assisted laser welding process (laser power 3.6 kW; welding speed 4.8 m/min). A — Top view; B — bottom view; C — cross-sectional view.

m^{-3}), d is the keyhole diameter, ν is the gas flow velocity, and C_d is the drag coefficient. The drag coefficient depends on Reynolds number.

Here, the slot Reynolds number is determined by the following equation (Refs. 24, 25):

$$Re = (\rho v d / \mu) \quad (2)$$

where μ is the dynamic viscosity of the gases (kg ms^{-1}) and ν is the gas flow velocity. The relationship between the drag coefficient and Reynolds number can be found in the handbooks of *Fluid Mechanics* for objects of several different shapes. In addition, the drag coefficient also can be experimentally measured. Here, we will not give a detailed discussion. For a given flow rate, the welding process using a smaller shielding gas nozzle cross section has a higher shielding gas velocity. According to Equation 1, a higher drag force is created by increasing the shielding gas flow rate, which not only drives the molten metal in the front of the keyhole to quickly flow back to the rear of the keyhole but also enables a portion of the zinc vapor to quickly escape from the bottom of the keyhole. In addition, the laser-induced plasma plume within and above the keyhole is suppressed by the side shielding gas. This factor helps to provide a consistent coupling between the laser-beam energy and the workpieces. As a consequence, the keyhole is enlarged and stabilized, through which the zinc vapor is continuously released without interrupting the molten pool.

Figure 4 shows the experimental results obtained by the recently developed method, which shows that a defect-free, lap joint with complete penetration was obtained. No spatter or porosity was observed in the welds. The surface of the weld is very smooth and complete joint penetration was achieved. As can be seen in the polished cross section of the weld presented in Fig. 4C, the grain size within both the weld zone and heat-affected zone (HAZ) is larger than those in the base material, as would be expected.

Compared to the stand-off distance of traditional laser cutting, up to 1.0 mm, the 10 mm stand-off distance of the nozzle in the cutting-assisted laser welding process is relatively large but is necessary in order to avoid direct removal of the liquid metal by the high pressure flow of the gas. An important point is that the gas flow rate should be controlled depending on the size of the nozzle, welding speed, and laser power. For the nozzle used in this study, the preferred shielding gas flow rate is in the range of 0.5 to 1.5 m^3/h, which is dramatically lower than that used in conventional laser welding. When the flow rate of shielding gas is greater than 1.5 m^3/h, the 0.8-mm-thick workpieces are typically cut into two. However, if the flow rate of the shielding gas is lower than 0.5 m^3/h, the drag force from the nozzle is not sufficient to enlarge and stabilize the keyhole resulting in the welding process once again becoming unstable.

Effect of Welding Speed

Welding speed plays a significant role on the weld quality of zinc-coated steels. There is very little published on successfully achieving high-quality welds in zinc-coated steels at welding speeds greater than 4 m/min. Therefore, in order to study the effect of welding speed upon weld quality, welds were made using the semi-cutting-assisted laser welding process with a range of welding speeds (3.0 to 5.4 m/min) and variable laser power settings (3.0, 3.6, and 4.0 kW).

Figure 5 is a collection of photos showing the quality of the experimental results. As can be seen, defect-free welds were obtained at the welding speeds of 3 and 4.8 m/min. However, when the welding speed was increased to 5.4 m/min, spatter adjacent to the weld and porosity in the weld were observed. In addition, the weld surface was irregular. At the low welding speed, the molten pool is relatively large and the solidification time is long allowing sufficient time for the zinc vapor to escape. As the welding speed is increased, the molten pool becomes smaller and a shorter solidification time is available for the zinc vapor to escape. Furthermore, at the higher welding speed, the direction of laser-induced plasma and plume, and the swelling in the molten pool fluctuate temporally and spatially at higher frequency than that at the lower welding speed (Ref. 22). Therefore, the zinc vapor has a greater probability to disturb the molten pool and the keyhole has a higher probability of collapsing. Furthermore, increasing the welding speed decreases the collapse time of the keyhole and transforms the keyhole from a cylindrical shape to a tapered shape (Ref. 26). The reduced size of the keyhole around the interface of the two metal sheets facilitates the entrapment and expansion of the zinc vapor inside the molten pool. Therefore, the molten pool becomes turbulent and results in the formation of severe spatter and porosity in the welds.

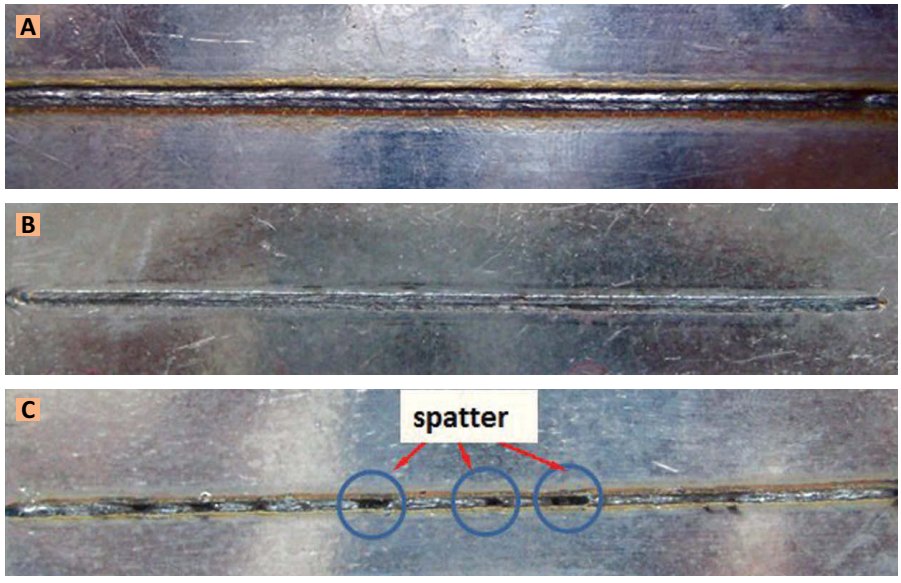

Fig. 5 — Comparison of weld quality at different welding speeds (top views of the obtained welds). A — 3.0 m/min; B — 4.8 m/min; C — 5.4 m/min.

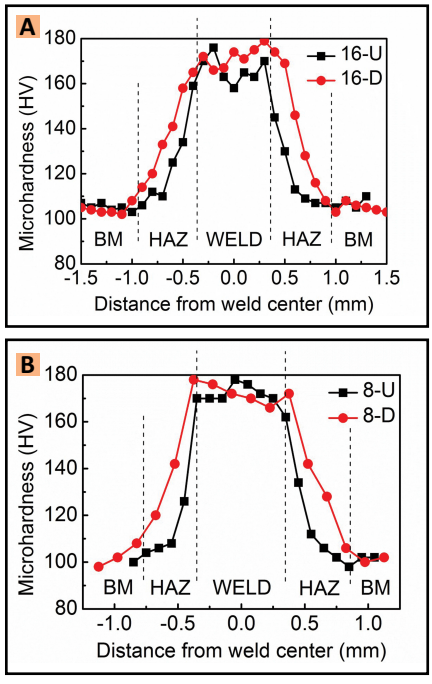

Fig. 6 — Microhardness profile of welds obtained at the following welding speed: A — 3 m/min; B — 4.8 m/min. (16-U: the hardness profile at the 0.3 mm depth from the top surface of sample 16; 16-D: the hardness profile at the 1.3 mm depth from the top surface of sample 16; 16-U: the hardness profile at the 0.3 mm depth from the top surface of sample 8; 16-D: the hardness profile at the 1.3 mm depth from the top surface of sample 8.)

Microhardness Test

The microhardness was analyzed along a profile from base metal through the weld back to base metal at increments of 0.1 mm and at a depth of 0.3 and 1.3 mm below the top surface of the weld. Figure 6A, B are graphical representations of typical microhardness distributions through the welds produced at welding speeds of 3 and 4.8 m/min, respectively. As can be seen in Fig. 6A, B, the base metal had a hardenss of approximately 100 HV and a maximum hardness of approximately 180 HV, which is located in the weld and is explained by the formation of martensite within the weld caused by the melting and rapid cooling after laser welding. No softening was found in the HAZ, and no effect of increasing weld speed was observed on the peak hardness value.

For low-carbon steels used in this study, there exist different types of ferrite in base metal, HAZ, and the weld zone, which have various morphologies. The variation in the ferrite's morphology results in different hardnesses at different zones. Base metal mainly contains the equiaxed ferrite. However, weld zones and HAZ mainly contain polygonal ferrite and the elongated columnar ferrite, respectively. Compared to equiaxed ferrite, there exists higher dislocation density and a large amount of subboundaries within the polygonal ferrite, thus exhibiting higher hardness value in the weld zone than that in the base metal (Refs. 27, 28). Also, the higher residual stress in HAZ leads to higher hardness (Ref. 28).

Tensile Test

Figure 7A is a plot of tensile properties from representative welds obtained at a welding speed of 3 and 4.8 m/min, respectively. It can be observed from Fig. 7C that the semi-cutting-assisted laser welded tensile samples fracture in the base metal and not in the weld zone or HAZ. However, the weld itself is very hard and constrains the total amount of deformation along the gauge length, resulting in comparable fracture strengths but lower total strains — Fig. 7A.

Conclusions and Future Work

The ability to laser weld zinc-coated steels in a zero root opening, lap-joint configuration with the assistance of a semi-cutting jet of shielding gas was studied in this work. Furthermore, the effects of welding speed on weld quality were investigated. Under the experimental conditions used, the following conclusions can be drawn:

1. The shielding gas nozzle applied directly to the top of the keyhole and the molten pool is redesigned. The critical modification is a reduced shielding gas nozzle cross-sectional area in order to increase the shielding gas velocity. It is found that for a gas at a given pressure level and temperature, the resulting drag force exerted on the molten pool and the keyhole stability is significantly enhanced by increasing the flow rate of the shielding gas used.

2. When the keyhole is enlarged and stabilized due to the increased drag force, the release of zinc vapor is improved. This improvement led to defect-free welds being achieved in a zero root opening, lap-joint configuration by use of the semi-cutting-assisted laser welding process at a welding speed of up to 4.8 m/min and a shielding gas nozzle cross section of 2 mm diameter.

3. The welding speed plays a significant role on the weldability of zinc-coated steels. The higher the welding speed, the more the instability of the welding process. It is demonstrated that the laser-induced plasma and plume direction changes significantly with the increased welding speed. The depth of penetration decreased with an increase in travel speed.

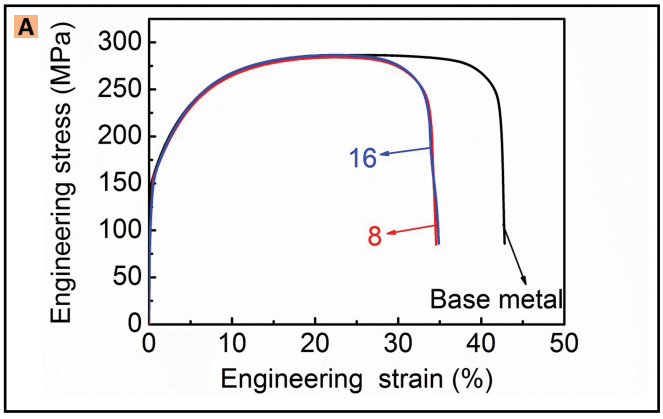

Fig. 7 — Tensile test results. A — Relationship between engineering stresses and engineering strain; B — fracture location of base materials; C — fracture location of typical welds.

4. The welds obtained by semi-cutting-assisted laser welding exhibit a greater weld strength, i.e. hardness, and negligible HAZ as compared to the base metal. Thus, under tensile shear loading, the base metal fractured before any fracture of the weld or HAZ.

5. The semi-cutting-assisted laser welding process is easy to operate in the production environment and meets the productivity requirements of the automotive industry.

As for future work, a correlation is needed between the laser power and the nozzle angle as well as the workpiece thickness. Furthermore, a high-speed camera with an illumination light will be used to monitor in real-time the dynamic behavior of the molten pool, the keyhole, and the laser-induced plasma and plume.

References

1. Graham, M. P., Hirak, D. M., Kerr, H. W., and Weckman, D. C. 1996. Nd: YAG laser beam welding of coated sheet steels using a modified lap joint geometry. *Welding Journal* 75(5): 162-s to 170-s.

2. Gu, H. P. 2010. Laser lap welding of zinc coated steel sheet with laser-dimple technology. *Journal of Laser Applications* 22(3): 87–91.

3. Lee, S. J., Katayama, S., Kawahito, Y., Kinoshita, K., and Kim, J. D. 2013. Weldability and keyhole behavior of Zn-coated steel in remote welding using disk laser with scanner head. *Journal of Laser Applications* 25(3): 032008/1–5.

4. Forrest, M. G., and Lu, F. 2004. Advanced dual beam laser welding of zinc-coated steel sheets in lap joint configuration with gap-free at the interface. *23rd International Congress on Applications of Lasers & Electro-Optics*, ICALEO.

5. Gu, H., and Mueller, R. 2011. Hybrid welding of galvanized steel sheet. *20th International Congress on Application of Lasers & Electro-Optics*, ICALEO, pp. 130–139.

6. Kim, C., Choi, W., Kim, J., and Rhee, S. 2008. Relationship between the welding ability and the process parameters for laser-TIG hybrid welding of galvanized steel sheets. *Materials Transactions* 49(1): 179–186.

7. Xie, J., and Denney, P. 2001. Galvanized steel welding with lasers. *Welding Journal* 80(6): 59–61.

8. Milberg, J., and Trautmann, A. 2009. Defect-free joining of zinc-coated steels by bifocal hybrid laser welding. *Production Engineering: Research and Development* 3(1): 9–15.

9. Iqbal, S., Gualini, M. M. S., and Rehman, A. U. 2010. Dual beam method for laser welding of galvanized steel: experimentation and prospects. *Optics & Laser Technology* 42(1): 93–98.

10. Chen, W., Ackerson, P., and Molian, P. 2009. CO_2 laser welding of galvanized steel sheets using vent holes. *Materials and Design* 30: 245–251.

11. Wang, P. C., and Hou, W. K. Method of joining galvanized steel parts using lasers. United States Patent 6,646,225.

12. Dasgupta, A., Mazumder, J., and Bembenek, M. 2000. Alloying based laser welding of galvanized Steel. *19th International Conference on Applications of Lasers & Electro Optics*, Laser Institute of America, Dearborn, Mich., October.

13. Li, X., Lawson, S., and Zhou, Y. 2007. Novel technique for laser lap welding of zinc coated sheet steels. *Journal of Laser Applications* 19(4): 259–264.

14. Pennington, E. J. 1987. Laser welding of galvanized steel. United States Patent 4,642,446.

15. Williams, S. W., Salter, P. L., Scott, G., and Harris, S. J. 1993. New welding process for galvanized steel. *26th International Symposium, Laser Applications in the Automotive Industries*, 49–56.

16. Yang, S. L., and Kovacevic, R. 2009. Laser welding of galvanized DP980 steel assisted by the GTAW preheating in a gap-free lap joint configuration. *Journal of Laser Applications* 21(3): 139–148.

17. Yang, S. L., and Kovacevic, R. 2009. Welding of galvanized dual-phase 980 steel in a gap-free lap joint configuration. *Welding Journal* 88(8): 168-s to 178-s.

18. Ma, J. J., Kong, F. R.,Carlson, B., and Kovacevic, R. 2013. Two-pass laser welding of galvanized high-strength dual-phase steel for a gap-free lap joint configuration. *Journal of Materials Processing Technology* 213(3): 495–507.

19. Yang, S. L., Kovacevic, R., and Carlson, B. E. 2011. Laser welding of high-strength galvanized steels in a gap-free lap joint configuration under different shielding conditions. *Welding Journal* 90(1): 8-s to 18-s.

20. Mitsubishi Co. 1993. US Patent 5618425.

21. Tzeng, Y. F. 1999. Pulsed Nd:YAG laser beam welding of zinc-coated steel. *Welding Journal* 78(7): 238-s to 244-s.

22. Yang, S. L., Wang, J. F., Carlson, B. E., and Zhang, J. 2013. Vacuum-assisted laser welding of zinc coated steel in a gap-free lap joint configuration. *Welding Journal* 92(7): 197-s to 204-s.

23. Ion, J. C. 2005. *Laser Processing of Engineering Materials: Principles, Procedure and Industrial Application*, Butterworth-Heinemann, Mass., Chapter 14.

24. Chen, S. L. 1999. The effects of high-pressure assistant-gas flow on high-power CO_2 laser cutting. *Journal of Materials Processing Technology* 88: 57–66.

25. Binder, R. C. 1973. *Fluid Mechanics*, 5th ed., Prentice-Hall, Englewood Cliffs, N.J., Chapter 5.

26. Ducharme, R., Kapadia, P., and Dowden, J. 1993. The collapse of the keyhole in the laser welding of materials. *12th International Conference on Applications of Lasers & Electro Optics* 77: 177–183.

27. Krauss, G., and Thompson, S. W. 1995. Ferritic microstructures in continuously cooled in low- and ultra-low carbon steels. *ISIJ International* 35: 937–945.

28. Mukhopadhyay, G., Bhattacharya, S., and Ray, K. K. 2009. Strength assessment of spot welded sheets of interstitial free steels. *Journal of Materials Processing Technology* 209: 1995–2007.